Biochimie 177 (2020) 198–212

Contents lists available at ScienceDirect

Biochimie

journal homepage: www.elsevier.com/locate/biochi

Interaction of *N*-succinyl-diaminopimelate desuccinylase with flavonoids

Manuel Terrazas-López, Naún Lobo-Galo, Luis G. Aguirre-Reyes, Jorge L. Cuen-Andrade, Laura A. de la Rosa, Emilio Alvarez-Parrilla, Alejandro Martínez-Martínez, Ángel G. Díaz-Sánchez*

Departamento de Ciencias Químico-Biológicas, Instituto de Ciencias Biomédicas, Universidad Autónoma de Ciudad Juárez, Ciudad Juárez, Chihuahua, CP 32310, Mexico

ARTICLE INFO

Article history:
Received 25 September 2019
Received in revised form
3 August 2020
Accepted 21 August 2020
Available online 27 August 2020

Keywords:
N-succinyl-diaminopimelate desuccinylase
M20 peptidases
Metal binding groups
Flavonoids
Molecular docking

ABSTRACT

DapE is an enzyme that belongs to the *meso*-diaminopimelate/Lysine pathway. It is recognized as an antimicrobial target, hence compounds that inhibit its catalytic activity are required. The principal features considered in the selection of potential inhibitors for this enzyme are compounds containing metal binding groups that could block access of the substrate to the Zinc metal centers and/or block the assembly of the oxyanion hole. We show the interaction of DapE from *Enterococcus faecium*, *Staphylococcus aureus*, *Klebsiella aerogenes*, *Pseudomonas aeruginosa* and *Escherichia coli* with flavonoids: quercetin, catechin, luteolin, rutin and hesperidin. Flavonoids contain several oxygen atoms distributed along their structure in a pattern that may be considered for the development of new antibiotics. Docking experiments suggest that these compounds containing metal binding groups that interact with metal centers of DapE and binding experiments indicate that glycoside flavonoids are preferred by DapE.

1. Introduction

The *meso*-diaminopimelate/L-Lysine biosynthetic pathway provides key antimicrobial targets for bacterial control using specific inhibitors [1]. One of the most studied enzymes of this pathway is *N*-Succinyl-L,L-diaminopimelate desuccinylase (DapE: E.C. 3.5.1.18) [2–21], which catalyzes the production of L,L-diaminopimelate and succinate from *N*-Succinyl-L,L-diaminopimelate (NSDAP) [3]. DapE is a dimeric Zn^{2+}-dependent metallohydrolase [5,22] that requires a major conformational change during catalysis for the proper formation of an oxyanion hole, essential to stabilize the tetrahedral intermediate of the reaction [9,23]. The two Zn^{2+}-metals centers and the oxyanion hole assembly are the most promising structural features of the enzyme that must be considered in the development of new inhibitors. The known DapE inhibitors are small molecules containing metal binding groups (MBG), such as thiols containing compounds [4,7,11,13,21]; boronic acid derivatives [21]; phenyl derivatives [21], phosphate derivatives [21] and, indole derivatives [12,13]. Although there are considerable structural details of the DapE active site alone or in interaction with inhibitors [5,7,13,18,24,25], there are yet to be resolved more detailed structural features that could facilitate the selection of those MBGs, which at the end may be key in the design of new inhibitors. In the present report, we first identify a selective group of flavonoids as potential DapE ligands by means of virtual screening and report whether DapE from five opportunistic pathogenic bacteria (*Enterococcus faecium*, *Staphylococcus aureus*, *Klebsiella aerogenes*, *Pseudomonas aeruginosa*, and *Escherichia coli*) are capable of interacting with this type of polyphenols, a group of compounds known for containing MBG. The five selected bacteria are members of a group recognized as responsible of most intra-hospital acquired multidrug resistant infections, the so called ESKAPE pathogens [26] and *E. coli* [27]. To understand which structural features of the different flavonoids appear to be critical determinants in their interaction with DapE enzymes, we inferred from the binding of five compounds with slight differences in the MBG geometric array. In previous works, we reported that these flavonoids inhibit pancreatic lipase, trypsin and α-amylase [28–30], and suggested nutritional applications; and now we show a potential use of these

* Corresponding author.
E-mail addresses: manuel.terrazas@uacj.mx (M. Terrazas-López), naun.lobo@uacj.mx (N. Lobo-Galo), guadalupe.aguirre@uacj.mx (L.G. Aguirre-Reyes), al154896@alumnos.uacj.mx (J.L. Cuen-Andrade), ldelaros@uacj.mx (L.A. de la Rosa), ealvarez@uacj.mx (E. Alvarez-Parrilla), alejandro.martinez@uacj.mx (A. Martínez-Martínez), angel.diaz@uacj.mx (Á.G. Díaz-Sánchez).

https://doi.org/10.1016/j.biochi.2020.08.016
0300-9084/

compounds in the identification of key groups in the interaction with DapE, a group of enzymes associated with antimicrobial control potential.

2. Material and methods

2.1. Materials

Polyphenols, culture media, salts and buffers were purchased from Sigma-Aldrich. Restriction enzymes were from New England Biolabs. Gene synthesis and plasmid constructs were acquired from Genscript. Hi-trap protein-chromatographic columns were acquired from GE Healthcare. *E. coli* Bl21 pLys-DE3 strain was from Promega.

2.2. Cloning, expression and purification of DapE recombinant enzymes

The DapE gene sequences from *E. faecium* (UniProtKB: A0A133CNA8), *K. aerogenes* (UniProtKB: A6TC94), *P. aeruginosa* (UniProtKB: B7UX27) and *E. coli* (UniProtKB: Q8XBE0) were cloned into the expression plasmid pET28b at the *Nde1* and *Xho1* restriction sites; and DapE from *S. aureus* (UniProtKB: Q6GF48) was cloned into the same plasmid, but at the *Nhe1* and *Xho1* restriction sites. The five recombinant enzymes were expressed and purified using the same protocol, which consists of overexpression in *E. coli* Bl21 pLys-DE3 strain transformed with the corresponding pET construct. Single colonies were inoculated into LB broth with the same antibiotic until the suspension reached stationary phase. For protein expression, saturated suspended bacteria were diluted in fresh LB with kanamycin and cultured at 37 °C with aeration (vigorous shaking at 220 rpm) until the suspension reached an OD_{600nm} of 0.5. At this point, protein expression was induced with 0.2 mM of IPTG for 16 h at 20 °C with the same shaking velocity. Subsequently, cells were harvested by centrifugation at 6000 rpm at 4 °C and the pellet resuspended in lysis buffer (50 mM potassium phosphate buffer, 50 mM of KCl, 0.05% v/v Triton X-100, 5% v/v of glycerol, 1 mM of 2-mercaptoethanol, 30 mM of imidazole at pH = 8.0) and stored at −20 °C until further lysis and purification. Cell disruption was performed by sonication on ice of thawed suspensions at 30% output intensity , in 30 s pulses and 30 s of rest for 2 h period. Finally, the lysate was centrifuged at 12,000 rpm for 45 min at 4 °C and the supernatant was filtered through a 0.45 μm syringe filter.

The cleared supernatant was loaded into a Ni^{2+} Hi-trap HP column previously equilibrated with lysis buffer supplemented with 30 mM imidazole, and washed with 10 vol of 50 mM potassium phosphate buffer, 300 mM of KCl, 5% v/v of glycerol, 1 mM of 2-mercaptoethanol and 30 mM of imidazole at pH 8.0. Proteins were eluted with the same previous buffer supplemented with 300 mM of imidazole. Protein fractions were analyzed by SDS-PAGE; and those that contained homogeneous DapE were pooled together and dialyzed using a 10 kDa Centricon® against 50 mM potassium phosphate buffer, 50 mM of KCl, 5% v/v of glycerol, 1 mM of 2-mercaptoethanol pH 8.0, and stored at −80 °C.

2.3. Fluoresce binding experiments

Polyphenols binding to DapE enzymes was monitored after apparent equilibrium by measuring changes in the intrinsic tryptophan fluorescence at 37 °C using a spectrometer (Fluostar Omega, BMG®). The five different DapE at 0.05 mg/mL were excited at 290 nm, and fluorescence intensity was recovered at 340 nm after an hour of incubation at 37 °C in the absence or presence of different concentrations of ligands: quercetin, catechin, luteolin, rutin and hesperidin. To discard changes in fluorescence produced by possible solvent effects, a control experiment was performed by adding volumes of the solvent in absence of ligand to protein samples. The fluorescence of polyphenols was neither measured nor considered in the study under the premise that excitation and emission spectra are distant of those used for monitoring protein tryptophan fluorescence [31–34]. Changes in fluorescence intensity were plotted against the ligand concentrations and fitted to Eq. (1) or (2).

Eq. (1): Fluorescence binding saturation,

$$\Delta FI = B_{max}*[ligand]/K_d + [ligand] \quad (1)$$

where ΔFI, is the change in fluorescence intensity at 340 nm; B_{max}, is the maximum ΔFI and corresponds to the maximum binding; [ligand], is the ligand concentration and K_d, is the dissociation constant.

Eq. (2): Fluorescence binding saturation with sigmoicity,

$$\Delta FI = B_{max}*[ligand]^h/K_d^h + [ligand]^h \quad (2)$$

where *h*, is Hill number and the other terms are the same as in Eq. (1).

2.4. Virtual screening for identification of potential DapE ligands

A virtual screening of compounds that potentially interact with DapE enzyme was performed using DockBlaster [35,36], and as target the crystalline structure of *Haemophilus influenzae* DapE (HiDapE) in the open conformation (PDB code: 3ic1)—The selection of HiDapE enzyme was based on the extensive structural studies available, which facilitate inference into related bacterial protein homologs. An automatic search for protein cavities was performed and the active site cavity was manually selected to perform the screening with HMDB (The Human Metabolome Database). The screening output consisted of 124 compounds, which included several polyphenols; and from which, two flavonoids (luteolin and rutin) were selected and their capacity to interact with DapE from the ESKPE enzymes was further tested and confirmed by means of AutoDock Vina docking and fluorescence binding experiments. After analyzing the flavonoids found in the docking, and based on our previous studies on digestive enzymes [28–30], we decided to additionally include quercetin, catechin and hesperidin in our subsequent studies, as explained below.

2.5. Molecular docking of selected flavonoids

After the selection of the five flavonoids, these were alternatively docked into the five ESKPE-DapEs three-dimensional homology models, as well as in HiDapE structure (for reference), using the AutoDock Vina software [37]. Flavonoids binding sites in DapE enzyme were inferred by means of docking experiments in ESKPE-DapEs models and HiDapE, in the open (PDB code: 3ic1) and the closed (PDB code: 5vo3) conformations. The nine best scored solutions were analyzed [37] and the one that is best fitted into the active site was taken as the binding model; notably, these best solutions frequently correspond to those where the flavonoid B ring is near to the metal centers. Ligand 3-D structures were downloaded from Zinc Database as follows: quercetin (code: 3869685) catechin (code: 119978), luteolin (code: 18185774) rutin (code: 59764511), hesperidin (code: 8382286). Three-dimensional structures were dock prepared using USCF-Chimera [38], followed by the function AutoDock Vina, which was used to perform docking using a grid that corresponds to the entire dimeric structure and a subsequent refinement-adjusting grid that corresponds to the

dimensions of active site groove. The most abundant auto-validated complex model was analyzed, and the best fitted model is presented. The best solution of the complex was selected to identify the amino acid residues that participate in interactions with flavonoids in the enzyme closed conformation. To consider potential interaction of polyphenols to the enzyme through water molecules, structural water molecules observed in the template crystal were manually added to protein-ligand complexes.

In addition, homology models of the open and closed forms for the five recombinant ESKPE enzymes were constructed using the SWISS-MODEL server [39] and five flavonoids dockings were performed using AutoDock Vina as previously described.

3. Results and discussion

3.1. Identification and selection of flavonoids that potentially bind into DapE enzymes

Selection of the ligands was conducted in two steps. First, flavonoids were selected by their potential to bind into DapE, inferred from a virtual screening approach, using the HiDapE model structure as the target (PDB code: 3ic1), as well as the Dock-Blaster tool [35] and the Zinc-HMDB-list. Secondly, we took into account the structural differences of distinctive types of flavonoids, identified according to their classification as flavonols, flavones, flavan-3-ol, flavone-glycosides. Using AutoDock Vina software, the selected ligands were then docked into the homology generated models of EfDapE, SaDapE, KaDapE, PaDapE, and EcDapE (ESKPE-DapE), as well as in HiDapE only for corroboration (Table 2). HiDapE was chosen as the target for the virtual screening step, under the premise that DapE inhibitors are universal, given the structural similarities present in this enzyme class and assuming that HiDapE ligands are also capable of interacting with DapE from the ESKPE bacteria. Although we used the HiDapE structure as a target, we validated whether these ligands also interact with ESKPE enzymes, as described below as evidence of their universality as DapE ligands.

While the DockBlaster tool has proven to accurately identify new potential ligands for any particular protein target, it requires confirmation and additional experimental validation in each case [35,40,41]. The energy scores calculated (kcal/mol) by the tool are based on a rapid search using the Dock 3.5 software [35], where each tested compound passes through a rapid steric fit filter, scored for electrostatic (ES) and van der Waals (VdW) complementarity and adjusted for partial ligand desolvation generated from solvent occlusion (Table 1). To calculate binding energy values with a closer approximation to reality, it is necessary to subsequently conduct additional docking optimization experiments or perform other more detailed computational methodologies, such as molecular dynamics simulations (for instance Ref. [11]). In the case of the present study, additional docking optimization was performed as described in the methods section. We found a list of 124 potential DapE ligands, including 22 flavonoids (Table 1). The obtained scores for flavonoids range from −85 to −35 kcal/mol; while the corresponding K_d values, calculated from these scores, are 5×10^{-46} to 2×10^{-9} M, which notably correspond to ligands with unrealistic extreme affinity. Therefore, binding ΔG must be obtained from other methods given that DockBlaster seems to be useful for the initial identification of probable ligands, but not for making comparisons between the scores for the different ligands; therefore, it is assumed a limited validity of the employed docking methods. From the 22 flavonoids, five flavonols, four flavan 3-ol, four flavones, one flavanone a, and eight flavonoid-glycosides were obtained. To investigate the capacity of the active site of DapE enzymes to interact with these different flavonoids, luteolin, which is a representative of flavones, and rutin, which is representative of flavonol glycosides, were selected from the output list. We selected luteolin and rutin because we have previously studied them concerning their interaction with digestive enzymes and not based on any discrimination criteria using the DockBlaster scores. However, scores for luteolin and rutin are not the highest obtained, nonetheless, they present a high VdW ΔG values, which suggests that these flavonoids show satisfactory geometric complementarity with DapE active site (Table 1).

To acquire more biochemical information about the binding capacity of flavonoids with DapE enzymes, in addition to the selection of luteolin and rutin and due to the availability of the other flavonoids; we included quercetin (a representative of flavonols), catechin (a flavan 3-ol) and hesperidin (a flavanone-glycoside) for subsequent binding assays. We decided to include them because they represent three other types of flavonoid compounds with distinctive patterns in their MBGs; and thus, their analyses conceivably contribute to enrich our understanding of the specificity of the interaction of these enzymes with their ligands. Relevant to the biological significance, these compounds share bactericidal or bacteriostatic effects at low micromolar doses by altering the cell wall function; quercetin can damage the cell wall of gram-positive bacteria [42]; catechins also alters the cell wall thickness [43]; luteolin destroys the cell wall integrity [44]; rutin inhibits cell wall synthesis [45] and finally, hesperidin possesses antibacterial properties [46]. Presumably, these five flavonoids must share essential molecular targets specifically involved in bacterial cell wall metabolism, and given that deletion of *dapE* is lethal [2], we infer that DapE may be the main target of inhibition by these compounds, Thus, representative compounds of flavonols (quercetin), flavan-3-ol (catechin), flavones (luteolin), and flavonoid glycosides (rutin a flavonol and hesperidin a flavanone) were used in the binding assays (Fig. 1).

3.2. Fluorescence binding experiments of flavonoids into DapE enzymes

The binding of the five selected flavonoids into purified recombinant DapE enzymes from five pathogenic bacteria (Fig. 2) was measured by monitoring changes in protein intrinsic tryptophan fluorescence (Fig. 3). The corresponding dissociation constants were determined by measuring protein fluorescence quenching; observed after the addition of each polyphenol to samples of DapE enzymes (Fig. 3A). The trend of the observed changes was analyzed employing a non-linear curve fit of the data to Eq. (1) or (2) (Fig. 3). The data-fit yields three binding parameters: the total fluorescence change associated with the enzyme saturation by its ligand (B_{max}), which can be interpreted as a measure of the conformational changes of the enzyme produced upon ligand binding; the dissociation constant (K_d); and B_{max}/K_d, that is related to the specificity of the enzyme for the ligand, which expresses a relative term of induced protein conformational change in relation to the affinity of the enzyme toward the ligand (Fig. 4). The change in protein autofluorescence produced upon binding is dependent on the flavonoid concentration used, but it does not vary significantly over the incubation time, which implies that the conformational change of the enzyme upon ligand binding is a fast step.

The observed trend of the saturations was hyperbolic, and data was best fitted to Eq. (1). However, in the binding saturation experiment of the glycosylated flavonoids, rutin and hesperidin presented a marginally sigmoidal saturation in the case of EfDapE; these data were fitted to Eq. (2) (with Hill coefficients ≅1.3), which could be indicative of an apparent binding cooperativity (Fig. 3E and F). It is not clear if sigmoicity is due to the presence of two thermodynamically connected sites or if this can be explained by

Table 1
Flavonoid compounds identified in the virtual screening that potentially interact with DapE enzymes.

Flavonoid	ZINC Code number	Classification	score[a] (kcal/mol)	Number of contacts[b]	ES score[c] (kcal/mol)	VdW score[d] (kcal/mol)	Desolvation[e]: p/ap (kcal/mol)
Peonidin	00897727	Flavonol	−85.24	5	−88.08	−16.32	18.01/1.16
Cyanidin	03775158	Flavonol	−83.35	5	−81.60	−19.20	16.27/1.18
Delphinidin	03777403	Flavonol	−81.45	5	−81.76	−20.96	19.03/2.23
Glisoflavanone	05854562	Flavanone	−61.68	5	−44.96	−21.57	3.52/1.32
A glycoside-flavone	85552319	Glycoside-flavone	−54.78	6	−40.57	−23.01	5.27/3.53
Tamaraxetin	06484598	Flavan-3-ol	−48.97	5	−25.94	−29.56	4.80/1.74
Tamaraxetin	06484599	Flavan-3-ol	−47.18	5	−26.97	−26.91	4.75/1.95
Isorhamnetin	00517261	Flavonol	−44.68	4	−24.48	−23.93	3.73/0.01
Genistein	18825330	Flavone	−39.40	3	−20.72	−23.08	4.78/-0.38
Tamaraxetin	06484601	Flavan-3-ol	−38.92	5	−29.77	−15.97	4.52/2.31
Luteolin	18185774	Flavone	−38.00	4	−17.08	−26.21	5.01/0.27
Daidzein	18847034	Flavone	−37.72	3	−19.97	−20.51	3.60/-0.84
Tamaraxetin	06484602	Flavan-3-ol	−37.17	5	−25.25	−19.06	4.65/2.49
Epigallocatechin	03870412	Flavone	−35.92	5	−21.76	−19.60	4.09/1.35
Myricetin	03874317	Flavonol	−35.18	5	−17.99	−23.31	4.28/1.84
Apigenin 7-[galactosyl-(1->4)-manoside] variant	85734818	Flavone-glycoside	−61.00	6	−42.41	−28.50	5.50/4.41
A glycoside-flavone	33963983	Flavone-glycoside	−54.10	6	−43.25	−23.25	6.69/5.70
Apigenin 7-[galactosyl-(1-> 4)-manoside] variant	85734820	Flavone-glycoside	−53.49	6	−38.14	−27.06	8.06/3.65
A glycoside-flavone	85552314	Flavone-glycoside	−52.64	6	−38.07	−22.93	4.74/3.62
Apigenin 7-[galactosyl-(1-> 4)-manoside] variant	85734832	Flavone-glycoside	−49.07	6	−39.54	−18.70	4.46/4.71
Apigenin 7-[galactosyl-(1-> 4)-manoside] variant	85734826	Flavone-glycoside	−48.34	6	−44.63	−12.50	3.79/5.00
Rutin	04096846	Flavonol-glycoside	−48.27	5	−34.26	−21.80	4.26/3.53

[a] DockBlaster score.
[b] Number of polar contacts.
[c] Physics-based scoring function borrow forcefield derived term for electrostatic complementary Score.
[d] Physics-based scoring function borrow forcefield derived term for van der Waals complementary Score.
[e] Desolvation score, polar electrostatic component (P), and apolar component due to dispersion, hydrophobicity, and cavitation (ap).

the existence of a slight heterogeneity in the binding sites; regardless of which mechanism is taking place, we presume that the carbohydrate moiety of these ligands may be responsible for the effect. Given that these Hill number values are near to one, we re-analyzed the data by fixing this parameter to one in Eq. (1) (gray line in Fig. 3E and F) and observed a suitable fitting, with results that were similar to those obtained by leaving the parameter free. Although, the fitting to a sigmoidal model is better than that of a hyperbolic, we do not know if the observed sigmoicity is significant and its validation requires further experiments.

3.2.1. Change in intrinsic fluorescence after flavonoid binding

DapE has been observed in multiple conformational states ranging from a compact form (closed conformation) to an extended form (open conformation); therefore, it has been inferred that DapE may exist in equilibrium between these two forms [9,23]. The transition from the open to the closed form is essential for the optimal enzyme activity, since conformational changes associated to this transition result into the assembly of the oxyanion hole, necessary to stabilize the tetrahedral intermediate formed during the catalysis, after the attack of the hydroxide ion over the carbonyl of the substrate [23]. Thus, it is expected that ligand binding into

Table 2
Docking scores of flavonoids into ESKPE-DapE enzymes.

	HiDapE		EfDapE		SaDapE		KaDapE		PaDapE		EcDapE	
	Open	Closed	Open	Closed	Open	Closed	Open	Closed	Open	Closed	Open	Closed
Template	3ic1	5vo3	4ppz	5vo3	4ppz	5vo3	4ppz	5vo3	4ppz	5vo3	4ppz	5vo3
Identity (%)	100	100	23.35	25.76	23.85	22.47	56.12	62.30	59.09	56.00	56.38	61.50
Model score (GMQE[a])	0.99	0.99	0.65	0.67	0.60	0.61	0.83	0.86	0.80	0.82	0.83	0.85
Model score (QMEAN[b])	1.34	1.64	−3.24	−2.93	−5.12	−3.79	0.49	0.91	0.79	0.10	0.33	0.43
Docking Score energy (kcal/mol)												
Quercetin	−6.3	−7.80	−7.80	−8.20	−7.60	−7.50	−4.90	−8.10	−8.10	−7.70	−8.00	−8.10
Cathechin	−6.4	−6.90	−7.10	−8.20	−7.20	−6.60	−4.70	−7.20	−7.60	−7.20	−7.20	−7.10
Lutheolin	−6.5	−7.70	−7.80	−8.30	−7.50	−8.30	−4.40	−7.70	−8.30	−7.40	−8.30	−7.60
Rutin	−5.9	−7.00	−8.40	−8.40	−9.40	−7.20	−2.10	−6.00	−8.40	−8.30	−8.70	−6.70
Hesperidin	−7.4	−8.80	−8.80	−9.00	−9.20	−8.20	−6.90	−3.00	−9.10	−7.60	−10.00	−5.90

[a] GMQE is for Global Model Quality Estimation. Good models are values close to 1, reflecting the expected accuracy of a model built with that alignment and template and the coverage of the target.
[b] QMEAN is for Quality Mean. QMEAN Z-scores around zero indicate good agreement between the model structure and experimental structures of similar size. Scores of −4.0 or below are an indication of models with low quality.

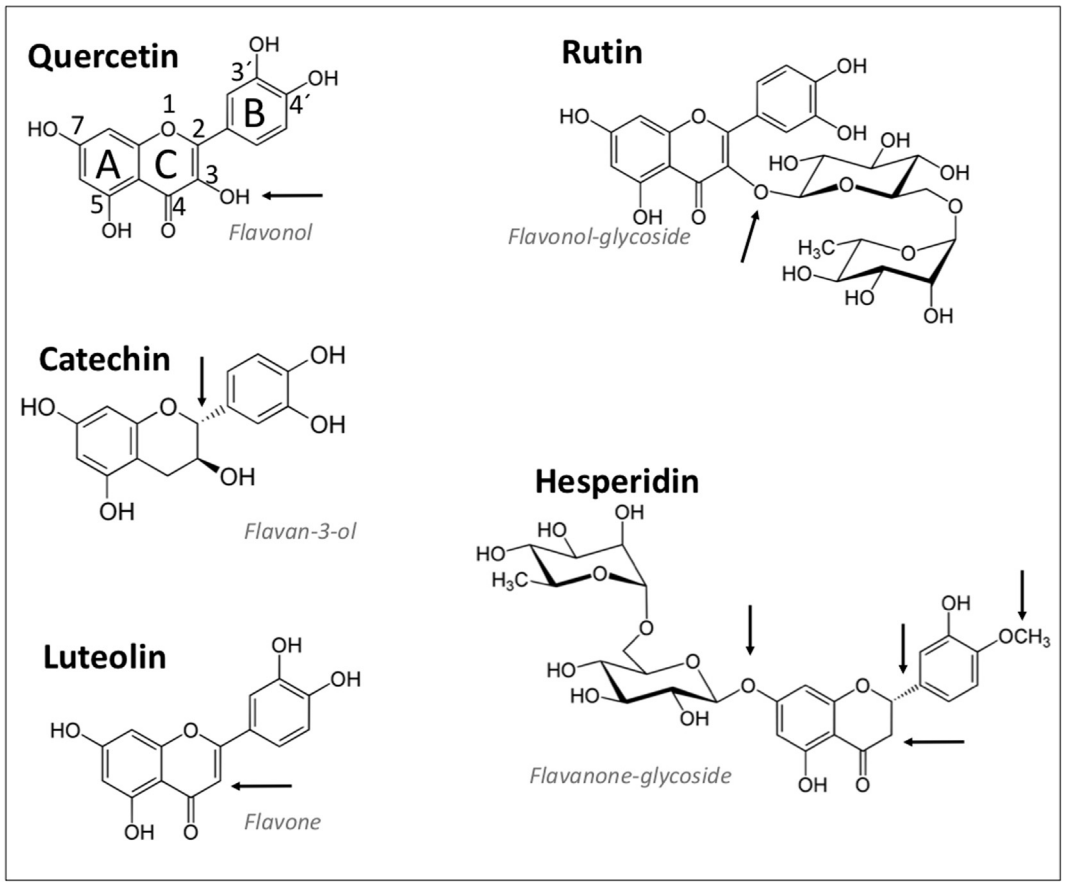

Fig. 1. Structure of used flavonoids compounds. Arrows indicate the differences between compounds, position numbers, and ring letters over quercetin are depicted. Structures were elaborated using ChemScketch®.

DapE active site favors this conformational transition, and consequently, this change may be monitored using sensitive spectroscopic techniques, as it is the case with tryptophan fluorescence. Quenching of intrinsic protein fluorescence upon ligand binding is commonly accepted as evidence of a protein conformational change. In the case of DapE, this change could be associated to the transition from the open to the closed conformation. In this regard, we found that binding of flavonoids in ESKPE enzymes produced a quenching in the intrinsic tryptophan fluorescence, as shown in the case of quercetin binding in EfDapE (Fig. 3A). Apparently, catechin

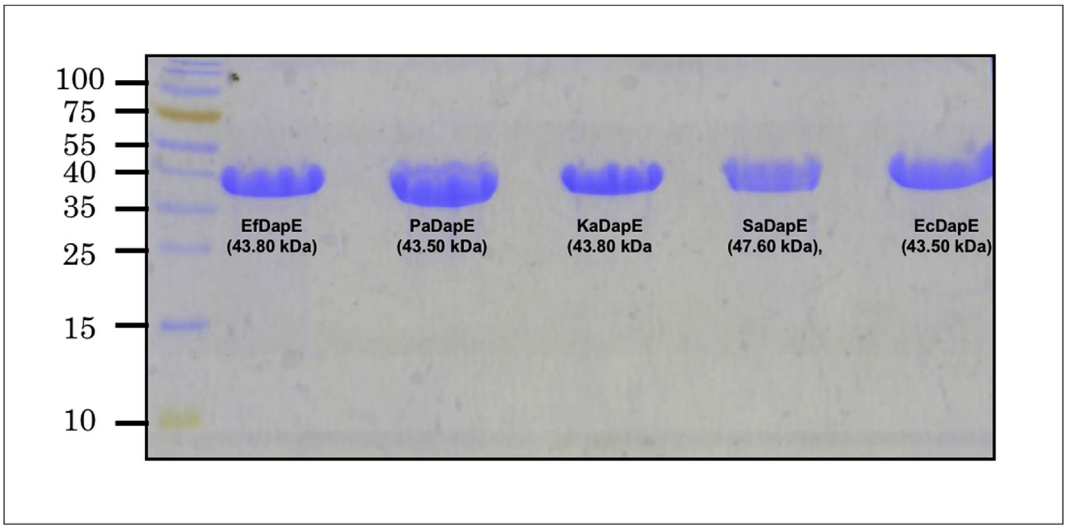

Fig. 2. Purification of recombinant DapE enzymes. Coomasie-stained-SDS-PAGE of purified fractions loaded as indicated in the picture: molecular weight standards and DapE from *E. faecium* (EfDapE); from *P. aeruginosa* (PaDapE); *K. aerogenes* (KaDapE); *S. aureus* (SaDapE) and *E. coli* (EcDapE), respectively.

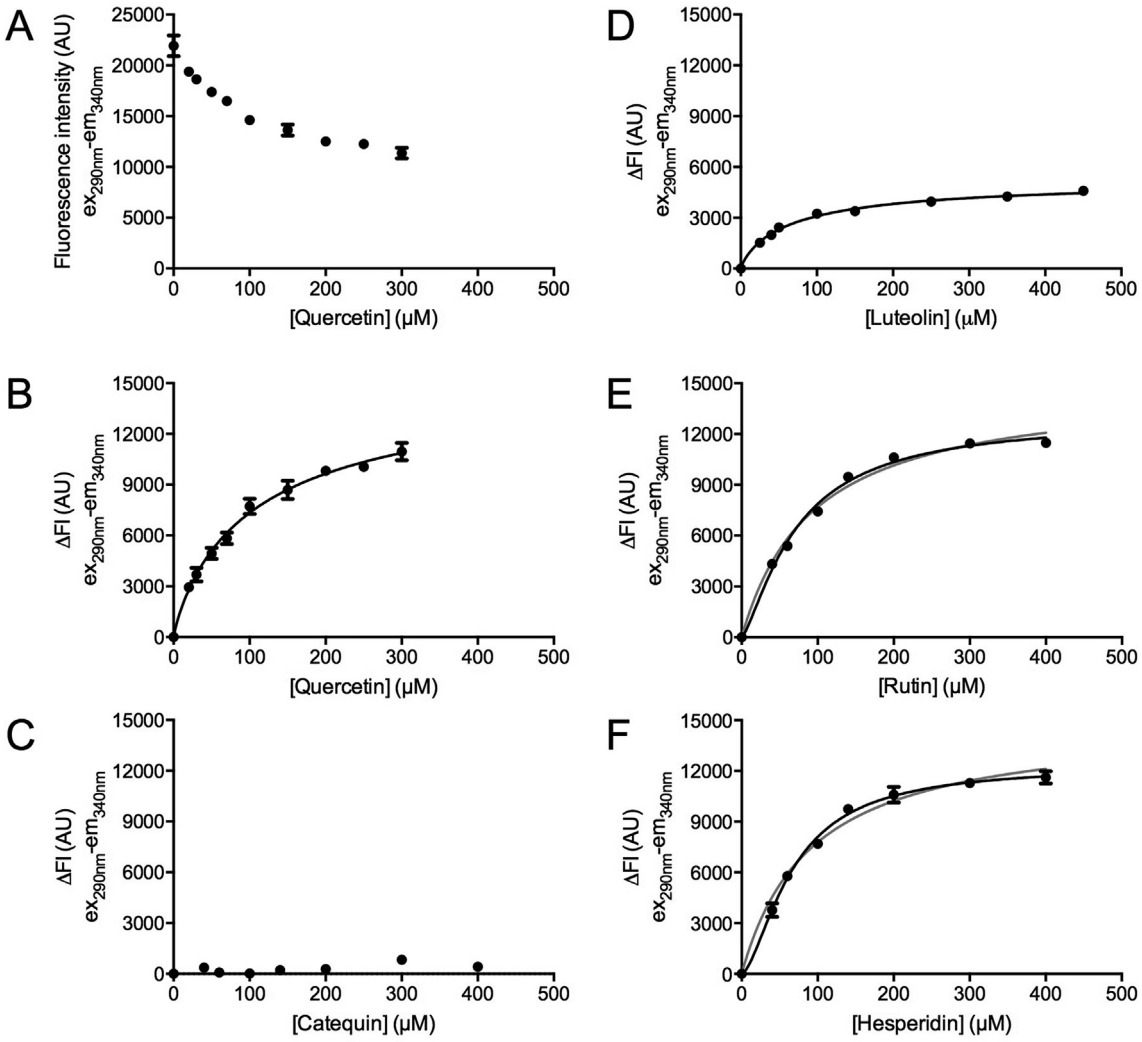

Fig. 3. Flavonoids binding equilibrium experiments into DapE. The five recombinant enzymes were assayed with the five ligands at least in three independent experiments and for clarity, only the data for EfDapE enzyme are presented. (A) Binding saturation experiment of EfDapE with quercetin showing the tryptophan intrinsic fluorescence intensity against the ligand concentration. Change in fluorescence intensity (ΔFI) observed in the binding saturation with (B) Quercetin; (C) Catechin; (D) Luteolin; (E) Rutin and (F) Hesperidin. Data standard error bars are shown for the change of intrinsic fluorescence obtained recording fluorescence at 340 nm and exiting with 290 nm (ex_{290nm}-em_{340nm}). Data were plotted and analyzed with GraphPad Prism 5.0® using Eq. (1) (black lines)or (2) (gray lines in (E) and (F)).

was unable to bind into the recombinant DapE enzymes (Fig. 3C; 4A-C and E), with the exception of PaDapE (Fig. 4D). This observation is probably due to the absence of the double bond in C2 carbon of C ring in catechin (Fig. 1), which produces a relative more flexible ring, resulting in a different spatial arrangement of its MBG; and thus, affecting its fitness into the active site of ESKE-DapEs. Another possibility is that the catechin can bind to these enzymes, but that the signal we are monitoring does not detect their interactions. Ligands binding into EfDapE (Fig. 4A), and hesperidin binding into SaDapE (Fig. 4B), produced a greater change in fluorescence intensity compared to other DapE complexes (Fig. 4). In this regard, the two enzymes that presented an apparent greater conformational change or a larger induced fit, corresponds to those representatives of Gram-positive bacteria (Fig. 4A and B); and so, these results could be associated to differences in structure or critical amino acids between DapE enzymes of Gram-positive organisms and those of Gram-negatives. For instance, DapE of Gram-positive *E. faecium* contains two insertions in the oligomerization domain: one of four amino acid residues between positions 226 and 227; and another of five residues between positions 284 and 285. Although SaDapE presents only the first insertion, this is larger, consisting of 26 residues, of which five are residues of K, three of D and three of E. These charged amino acids rich areas in proteins are characteristic of intrinsically disordered regions. These inserts could account for the largest conformational changes observed, since they are located in loops that could not be easily modeled. Conceivably, it can be assumed a high probability that these disordered regions are stabilized upon ligand binding.

3.2.2. *Observed dissociation constants for the flavonoids*

The K_d values observed in this study ranged from submicromolar to micromolar level (Fig. 4). We found K_d values within three ranges: a relatively high values, from 113 to 280 μM, observed for the complexes EfDapE-quercetin, KaDapE-rutin and PaDapE-catechin; another group corresponding to relatively low values from 0.6 to 11 μM, which included complexes of SaDapE-rutin, SaDapE-Hes, PaDapE-Hes, EcDapE-quercetin and EcDapE-luteolin; and finally, an intermediate range from 20 to 72 μM, observed in the rest of the complexes.

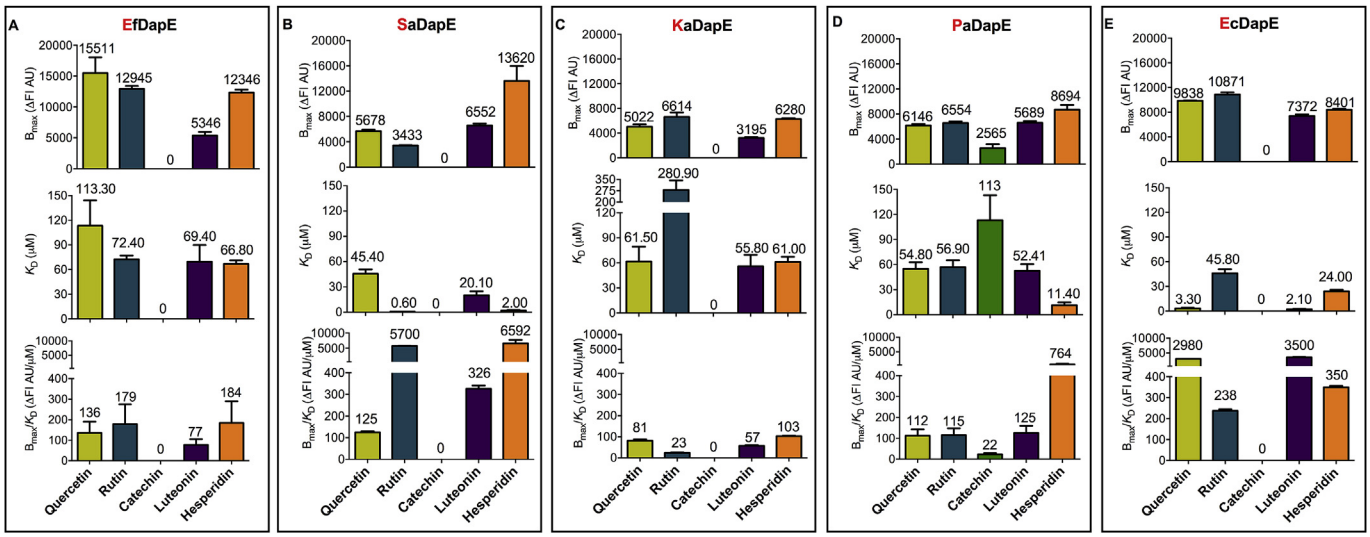

Fig. 4. Changes in flavonoids binding parameters of flavonoids into ESKPE DapE enzymes. Binding parameters obtained were replotted to illustrate the differences between ligands and enzymes: (A) EfDapE, (B) SaDapE, (C) KaDapE, (D) PaDapE and (E) EcDapE. Bars represent the standard error obtained in the non-linear fit to Eq. (1) of the three different binding experiments. Data were plotted and analyzed with GraphPad Prism 5.0®.

3.2.3. *Apparent flavonoid specificity*

In the case of EfDapE and KaDapE enzymes, comparable B_{max}/K_d values were observed for flavonoids, which may indicate that these enzymes have no preference for any of the polyphenols used (Fig. 4A and C). SaDapE has higher B_{max}/K_d values for glycosylated flavonoids: rutin and hesperidin (Fig. 4B), which is interpreted as a preference for glycosylated flavonoids, probably due to the carbohydrate moiety (Fig. 1). This observation is consistent with *in silico* inference analysis by Dock-Blaster that showed several potential ligands of glycoside nature (data not showed). B_{max}/K_d values in PaDapE were similar to those of EfDapE and KaDapE except for hesperidin, which was fivefold higher in complex with PaDapE (Fig. 4D), suggesting that this enzyme has a preference for flavanone glycosides. EcDapE B_{max}/K_d for quercetin and luteolin are almost 10 times higher than those observed in complex with rutin and hesperidin, implying that this enzyme prefers flavonols and flavanones (Fig. 4E).

3.3. *Flavonoids binding models*

Although there are extensive details regarding architecture of DapE and the role of residues that are essential for catalysis [2–21,23–25], as well as its interaction with inhibitors [4,6,7,11], this is the first study concerning the interaction of this enzyme with polyphenols. Moreover, the information concerning the structure of distant homologs, especially those of Gram-positive bacteria, is limited. To contribute to the understanding of the structural determinants of the binding of these ligands into DapE, molecular docking experiments of the flavonoids were performed using the tridimensional models of ESKPE-DapE enzymes (Fig. 5) (Table 2). These Docking analyses also serve to better connect our experimental results in a more consistent manner, and notably, to identify differences among ESKPE-DapE enzymes (Fig. 6). We also performed the molecular coupling of the flavonoids in the HiDapE as model reference, in both the open and closed conformation (Table 2 and Fig. 6). It was decided to use HiDapE as reference binding model, given the extensive crystallographic and biochemical data currently available for this enzyme, including structural information on the open and closed forms of its active site. In this regard, we first inferred the binding of flavonoids into ESKPE-DapEs and then confirmed them by docking assays in HiDapE. Finally, the information obtained about the residues that participate in the interaction with the ligands in the ESKPE enzymes were compared among themselves and with other DapE homologs. All tested ligands are geometrically and electrically compatible with the DapE active site regardless of the enzyme being analyzed on the open or closed conformation. We found that flavonoids bind to the active site pockets of DapE of the Gram-negative representatives (KaDapE, PaDapE, EcDapE, and HiDapE) via non-covalent bonds with metal centers and with multiple residues present in this cavity (Figs. 5 and 7A and D). Notably, the active site of these enzymes, specifically the substrate binding subsite (Fig. 7B), contains part of a loop that includes three highly conserved glycine residues (324–326, numeration of HiDapE hereafter used unless other is specified), which give enough space for the diaminopimelate moiety of substrate to accommodate in a productive position (Fig. 7B and C). G324 in KaDapE, PaDapE, EcDapE, as well as in HiDapE, also allow the accommodation of the B ring of the flavonoids ligands (Figs. 5 and 6D and E). In contrast, a residue change G324A was observed in EfDapE, which results in a reduction of the space of this pocket (Fig. 7C and E). Presumably, the methyl group of A324 in EfDapE interferes with the accommodation of B ring of flavonoids (Fig. 7E), but not with the entrance of the substrate (Fig. 7C). Therefore, in the docking of EfDapE, flavonoids are observed less buried inside the active site compared to the position observed in the ligand bound in the other enzymes (Figs. 5 and 7D). This difference apparently does not impact the equilibrium binding of these ligands into EfDapE, inferred from both, the parameters obtained in the fluorescence binding experiments (Fig. 4), as well as, the binding energies obtained in the docking results (Table 2). This could be explained by compensatory interactions observed between EfDapE and the ligands, in this case B ring of flavonoids does not form interactions with metal centers.

3.3.1. *Quercetin binding model*

Quercetin binds at the active site of the DapE model enzymes through polar interactions and by non-covalent bonds between metallic center 2 and flavonol B ring through cation-π interactions (Fig. 5A). The 4′-OH group interacts with E163 directly and via a bridge through the metal center 1. Residue Y197 is hydrogen

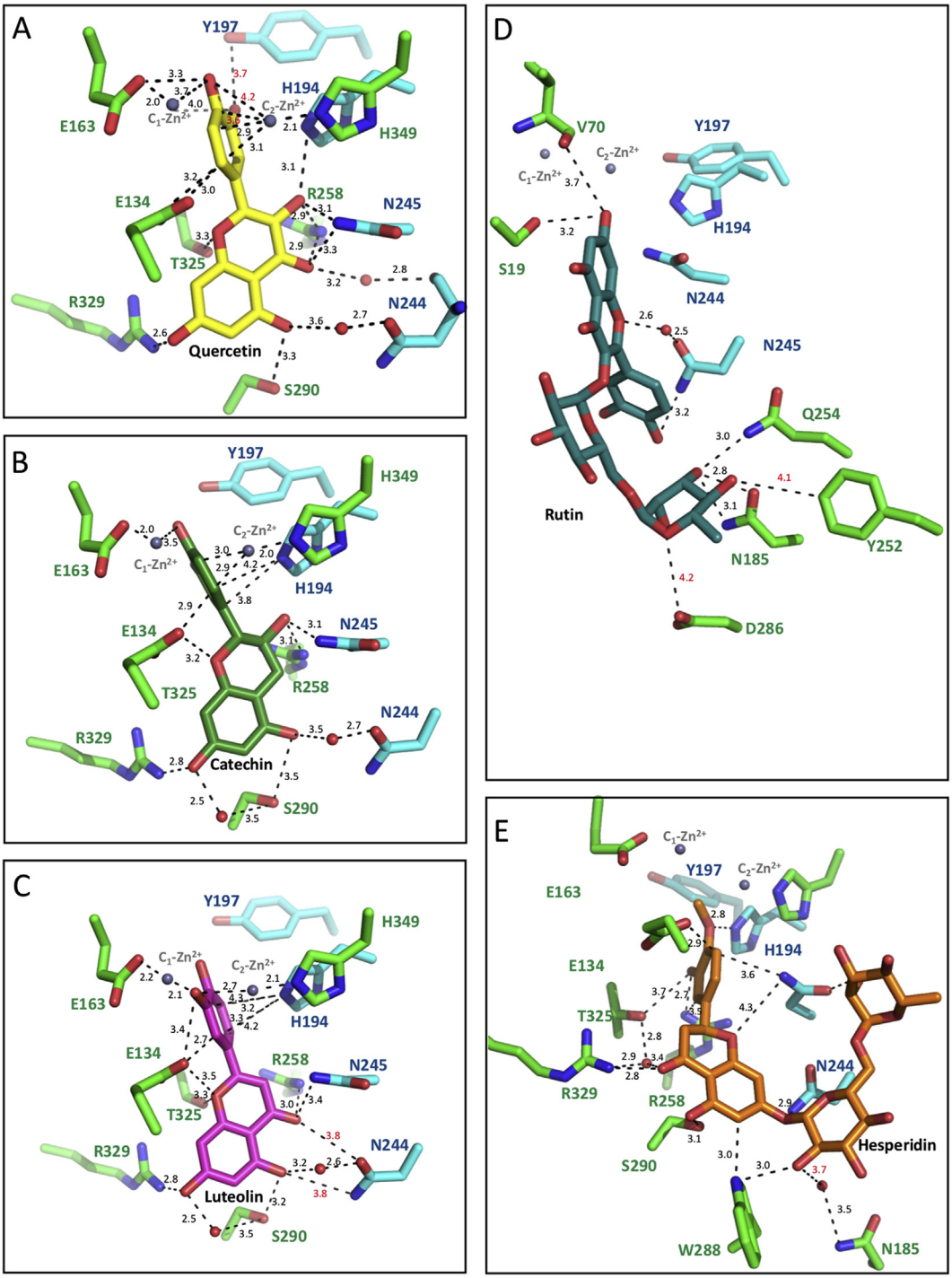

Fig. 5. Binding model of flavonoids into EcDapE. (A) Quercetin-EcDapE complex; (B) Catechin-EcDapE complex, (C) Luteolin-EcDapE complex; (D) Rutin-EcDapE complex and (E) Hesperidin-EcDapE complex models. Zn^{2+} ions are shown in ball representations, active site residues that potentially participate in binding are shown in stick representations. Flavonoids are depicted in sticks. Potential interactions between enzyme and ligands are shown as a dashed line with the distance in Å. All images were generated using PyMOL.

bonded to the OH 3′ group of B ring, while the carboxyl of E134 apparently stabilizes one of the positive dipoles of B ring by anion-π interaction. C ring is held by T325, which donates a hydrogen bridge to oxygen in position 1. R258 binds to the OH of position 3 and to oxo group 4. The N245 also interacts with these last two groups. N244 interacts trough a water molecule with OH-5 of A ring. The S290 interacts also with the OH-5 and with the OH-7 trough a water molecule, finally, OH-7 group is also bonded by R329.

In both, the open and closed models, quercetin binds in a similar manner, except that interactions with the B chain are absent since the corresponding residues are outside the binding distance and only present in proximity to the ligand upon induced fit. A general feature observed in the binding energies of flavonoids is that they are more favorable, in most cases, in the closed complexes compared to the open conformation, supporting the idea of an

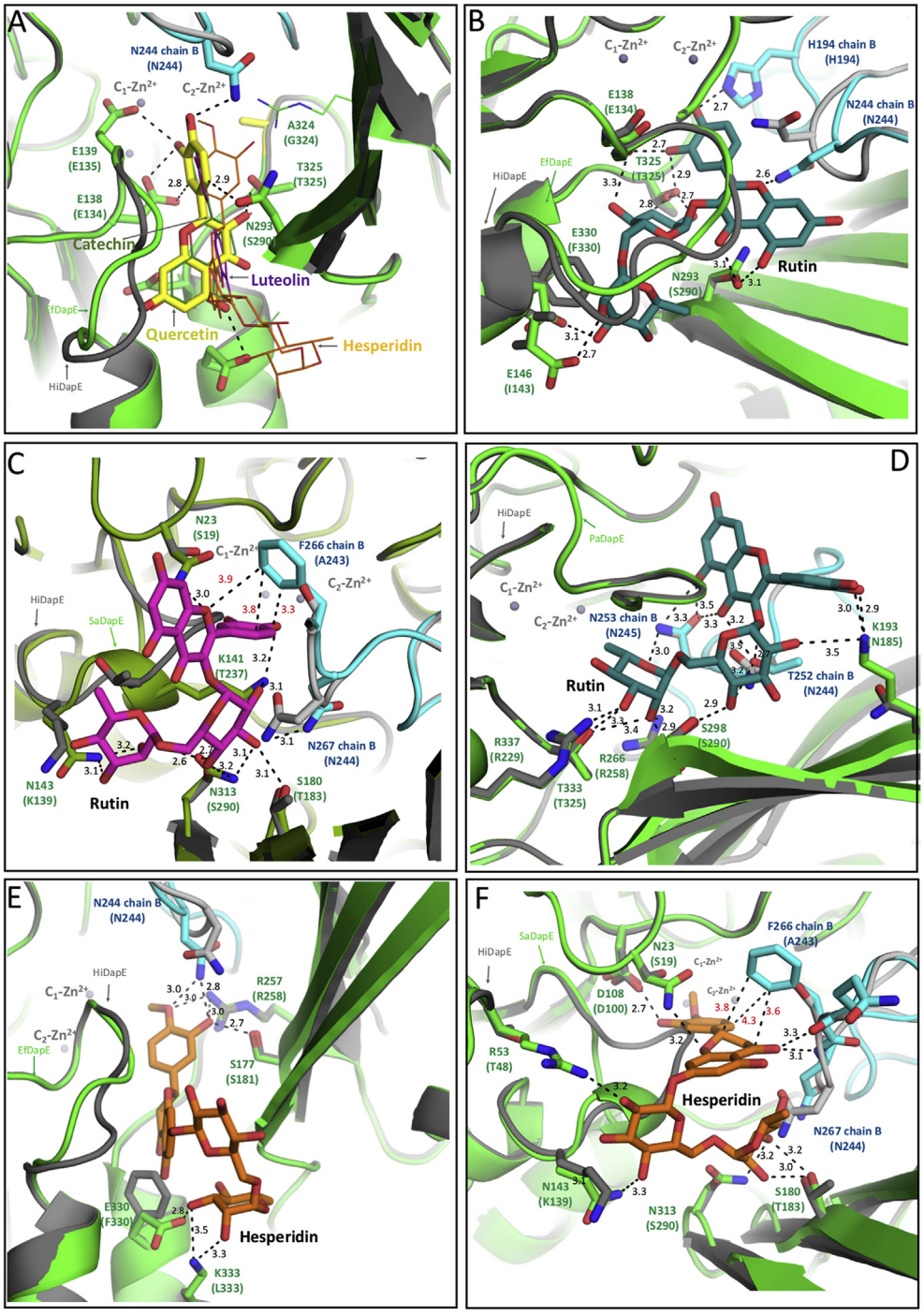

Fig. 6. Differences in binding of flavonoids into ESKPE-DapE enzymes. (A) EfDapE in complex with quercetin; and showing as reference the binding position of catechin, luteolin, and hesperidin. A324 is shown as yellow sticks. Interactions of EfDapE with hesperidin are shown in panel E. (B) EfDapE in complex with rutin. (C) SaDapE in complex with rutin. (D) PaDapE in complex with rutin. (E) EfDapE with hesperidin. (F) SaDapE in complex with hesperidin. DapE enzymes are shown as cartoon and relevant residues depicted in sticks. Black dashed lines represent polar interactions Images were obtained using PyMOL.

induced fit upon binding of the ligands. Unless otherwise indicated, all ligands bind similarly to the open or closed form of the DapE models used. In the case of quercetin binding in DapE-ESKPE, it was observed in a very similar position to the HiDapE-quercetin complexes. Although the fluorescence binding experiments of EcDapE showed consistently lower K_d values for ligands (Fig. 4E), compared to the other DapE enzymes, this enzyme does not show great differences in the positions identified as potentially critical in ligand binding. The exception is the presence of a W in position 288 in EcDapE, while smaller residues (D, P, A, and N) are observed in the ESP-DapE and HiDapE (Fig. 8A). This position is located in the entrance of the active site groove farther away from the bound ligands, thus, the role of this residues in the interactions with ligands requires further experiments, for instance, molecular dynamics simulations or site-directed mutagenesis.

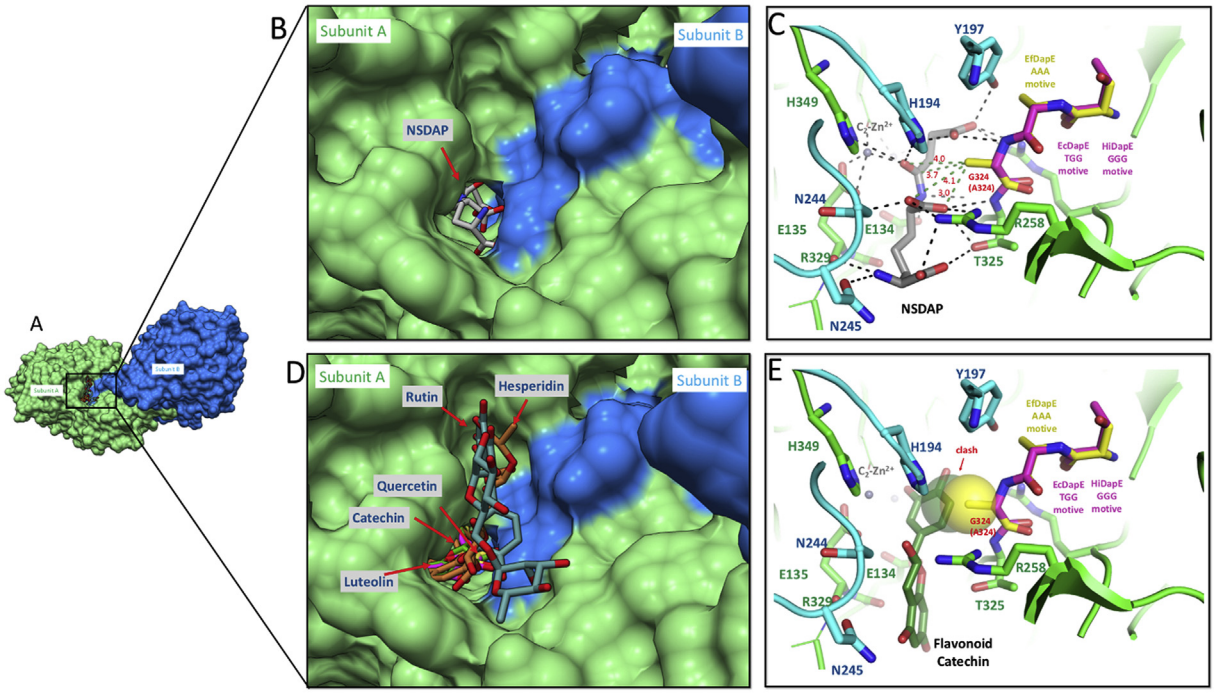

Fig. 7. Binding of flavonoids into EcDapE relative to substrate binding. (A) Dimeric structure of EcDapE enzyme model in the closed state showing the binding of flavonoid and NSDAP. (B) Docking of NSDAP into EcDapE active site groove. (C) Details of a different view of B, showing the binding interactions between enzyme and substrate. (D) Zoom view of A, showing the overlapping of ligands binding solution into active site. (E) A view of D, showing details of catechin binding as a representative complex to depict the entrance of flavonoids. NSADP and flavonoids are shown in sticks representation and EcDapE is depicted as surface in A, B, and D. EcDapE is shown as cartoon and relevant residues depicted in sticks. Black dashed lines represent polar interactions and green lines in C are depicted to show compatibility between active site GGG motive and NSDAP binding, contrary as shown in E, atoms depicted in transparent spheres show potential clash between A324 and flavonoids fully inside the groove. Images were obtained using USCF-Chimera.

3.3.2. *Catechin binding model*

Quercetin and catechin are very similar molecules, the difference resides in the C ring, which in catechin loses planarity due to the lacking of the double bond between carbons 2 and 3. In the binding models obtained, catechin is observed practically in the same position as in quercetin complex, with the exception of the loss of interaction with residue Y197 (Fig. 5B). N244 interacts with OH-5 of A ring through a water molecule, while S190 binds to OH-7 of the same ring via another water molecule. Paradoxically, while the structural determinants suggest that catechin should enter and bind to the active site cavity of EfDapE, SaDapE, KaDapE, and EcDapE, the fluorescence binding experiments did not provide evidence of these interactions.

3.3.3. *Luteolin binding model*

In the theoretical model of the luteolin binding, ligand is situated slightly more outward in the active site compared to quercetin, without losing any of the interactions with the same amino acid residues of the active site (Fig. 5C). Given that luteolin lacks the OH group at position 3′ of the B ring, further interactions between this flavonoid and the R258 and N245 residues are lost. Also, the interaction with Y197 and the cation-π interactions observed in quercetin with the metal center are also inferred, but these are instead performed with the H194 of B subunit. All other interactions are similar to those of quercetin. Two residual water molecules potentially participate in the luteolin binding. One of them bridges an interaction between N244 and OH-5 of A ring of the ligand and the other between S290 and OH-7 of the same ring. PaDapE has an S at position 244 while the other enzymes have an N. This change seems to allow an additional space in the active site cavity, which allows the A-B ring moiety to flip with respect to how luteolin is observed in the complexes of the other enzymes.

3.3.4. *Rutin binding model*

Rutin and quercetin are very similar flavonols, except for the presence of a disaccharide moiety at position 3 of C ring in rutin. It is expected that this moiety may results in a steric hindrance for the accommodation of rutin with respect to quercetin binding in DapE enzymes, and that was precisely what we found in the modeled complexes. The following describes a structural findings overview of the docking of this ligand and its relationship with the obtained experimental data. The binding pattern of rutin turned out to be the most different when compared to other ligands. Only B ring of the flavonoid moiety is inside the groove of active site of the EcDapE-model complex (Fig. 5D), and consequently, the main interactions between rutin and enzyme are observed with the carbohydrate moiety. A water molecule bridges an interaction between the N244 residue and the O1 of the flavonoid. Remarkably, rutin binds to DapE enzymes in a similar way, with the following differences. (1) The entry of the active site groove in EfDapE is slightly larger, due to the replacement F330E, allowing the carbohydrate moiety to accommodate deeper into the pocket, an accommodation that allows rutin to undergo additional interactions with this enzyme (Fig. 6B): the 4′-OH group of B ring interacts with H194 and the 3′-OH group performs two interactions, one with E138 (E134 in HiDapE) and the other with T325; the O1 of C ring receives a hydrogen bond from NH_2 of N244 and oxygen 4 and 5 of C and A rings, respectively, interacts with the amide of N293 (S290 in HiDapE); finally the carbohydrate moiety of the flavonoid interacts in a polar mode through their OH groups with the T325, E138, E330 and E146 (I143 of HiDapE). (2) In SaDapE rutin is observed in the same position as in complex with EcDapE, only that the flavonoid moiety is flipped, and B ring is located inside the active site groove (Fig. 6C). This difference may be due to the flip of the loops, one composed by residues from 133 to 137 and the other composed by

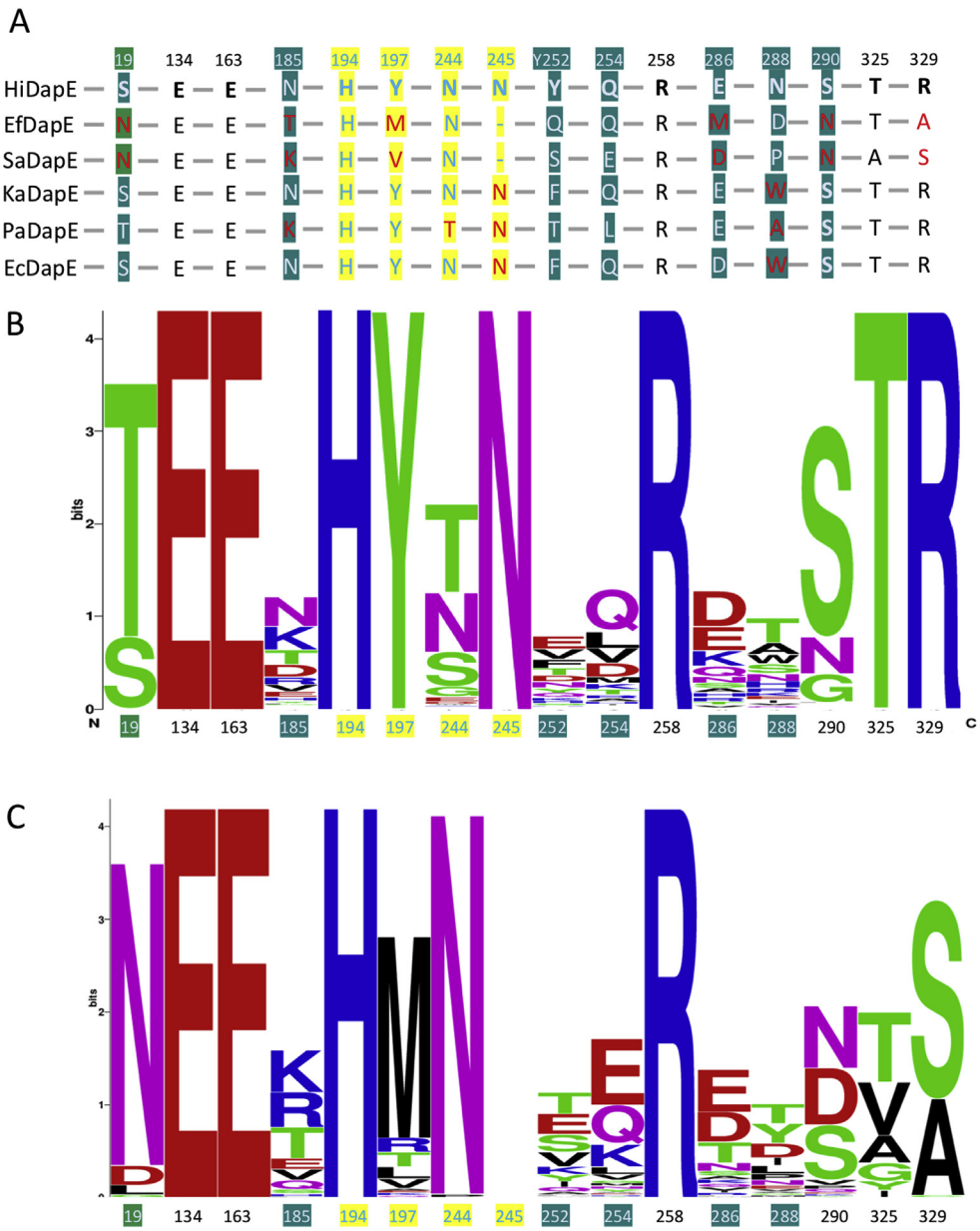

Fig. 8. Variability of residues potentially involved in flavonoid and substrate binding. (A) Alignment of residues between HiDapE and ESKPE DapE enzymes. (B) Frequency of residues potentially involved in flavonoid and substrate binding among the available DapE sequences from Gram-negative bacteria. (C) Frequency of residues potentially involved in flavonoid and substrate binding among the available DapE sequences from Gram-positive bacteria. The multiple alignment of DapE enzymes was used to plot frequencies in the logo image. The amino acid residues are depicted as color code based of their physicochemical properties as stated default it the WebLogo server (http://weblogo.berkeley.edu/logo.cgi: polar amino acids (G,S,T,Y,C,Q,N) are green, basic (K,R,H) blue, acidic (D,E) red and hydrophobic (A,V,L,I,P,W,F,M) are black).

residues 243 and 246, thus, allowing rutin B ring to enter into the active site groove of SaDapE and interacting with K141 (T137 of HiDapE), F266 (A243) of the B chain, by T-shape π-stacking interactions; F266 also interacts with C ring by the same type of contact; finally, the carbohydrate moiety of the ligand interacts through polar contacts with N143 (K139 from HiDapE), N313 (S290), S180 (T183), N267 (N244) of B chain of the dimer (Fig. 6C)—these structural differences of SaDapE could be related to the apparent higher affinity and also higher specificity observed in the equilibrium binding experiments (Fig. 4). (3) For PaDapE, rutin binds almost in the same position as in EcDapE and HiDapE, except that the flavonoid portion is rotated 180°, allowing the carbohydrate moiety to enter into the active site groove and perform the following interactions (Fig. 6D): K193 interacts with the 3′ and 4′ oxygens of the B ring and with the 2′-OH of residue 1 of the carbohydrate moiety; the side chain amide oxygen of N253 (245 from HiDapE) interacts with oxygen 4 and 5 of C and A ring, respectively; while the nitrogen of the same residue interacts with the oxygen 5 of A ring and with the oxygen of the pyranoside ring of the second carbohydrate residue; finally, R337 (R329), T333 (T325), R266 (R258), S298 (S290), and T252 (N244) perform polar contacts with the carbohydrate moiety.

3.3.5. *Hesperidin binding model*

Hesperidin is a glycosylated derivate of a flavanone at position 7 of A ring. Structurally, it is similar to catechin, with the difference that lacks the 3-OH group but instead contains a methoxy-group in 4′ carbon of B ring (Fig. 1). In the docking models, hesperidin

binding to DapE is similar to that of catechin, however, a 180° flip of A-C ring moiety is noticed in the complex model (Fig. 5E). This shift is stabilized by polar interactions with residues at the active site. The Glycosyl moiety of the ligand is hydrogen-bonded by S290, N244 and N245. Oxygens 4 and 5 of C and A rings, respectively, interacts with R329 and T325 via a residual water molecule; while another water molecule bridges an interaction between N185 and OH-3 from residue 1 of the carbohydrate moiety of the ligand. In EfDapE the change G324A causes hesperidin to adopt a different position to that observed in EcDapE, KaDapE, PaDapE, and HiDapE. Instead, it binds at the middle of the groove and produces the following interactions (Fig. 6E): the 4′-oxygen of B ring is linked by the OH group of S177 (S181 from HiDapE) and by R257 (R258), a residue that additionally participates in the stabilization of the 3′-oxygen together with the side chain of N244 (N244); also, the carbohydrate moiety of the ligand interacts polarly with residues E330 (F330) and K333 (L333). Finally, one of the loops located at the entrance of SaDapE active site presents some considerable changes. This variation alters the conformation of this loop with respect to that observed in the EcDapE model as well as in HiDapE crystal (PDB code: 5vo3). This loop is composed of residues ATAKD (136–140) in HiDapE and residues KEQEG (141–145) in SaDapE. From these, the variation of A136K prevents the flavonoid A and C rings to adopt the conformation observed in other DapE. Instead, in SaDapE A and C rings bind in an alternative position and performs the following interactions (Fig. 6F): F266 interacts with C ring and, in turn, oxygen 1 of this ring interacts with N23, just as O4 interacts with the peptide bond of N267 (244). The 3' oxygen of B ring is hydrogen bond to D108 (D100); the glyosidic portion performs polar interactions with R53 (T248), N143 (K139), N313 (S290), and S180 (T183).

3.3.6. Variability of amino acid residues potentially involved in flavonoid binding

The relative low amino acids sequence identities between DapE variants among the Gram-positive representative bacteria and those available in the PDB did not allow us to construct well-qualified homology models for EfDapE and SaDapE (Table 2). Given the low sequence identities, quality of the generated models, docking analysis (Table 2), and differences in experimental results (Figs. 3 and 4), it is conceivable that these two DapE enzymes presents distinctive structural and functional behaviors compared to those of Gram-negative representatives. Contrastingly, DapE enzymes of representative Gram-negative possess an apparent high degree of similarity among themselves. To extend our findings along the DapE enzymes available in the databases and to correlate the structural and biochemical features found in this study, a multiple amino acid sequence alignment of the ESKPE DapE homologs was performed and residues potentially involved in ligand specificity were analyzed (Fig. 8). In ligand-complex models KaDapE, PaDapE, and EcDapE as well as in HiDapE-ligand complexes, it was observed that quercetin, catechin, luteolin and rutin bind almost identically. The differences in binding parameters between the five recombinant enzymes observed in our experiments could be due to modest variations at the amino acid residues at these positions (Fig. 8A). We classify these potentially critical positions into the following types: (1) Highly conserved positions in DapE enzymes (E134, E163, R258, T325 and R329), encoded by ESKPE as well as in all the sequences available in GenBank database from both Gram-negative (Fig. 8B) and Gram-positive (Fig. 8C). We infer that these DapE residues are important for binding of the substrate and other ligands, as in this case, flavonoids, as well as for DapE functional properties, but do not determine ligand specificity. (2) Residues that enters the active site groove, located in the B subunit in the dimeric interface, which potentially interact with the ligands after the conformational change of the enzyme from the open to the closed form. These residues (H194, Y197 N244 and N245) are also present in almost all DapE enzymes available. Among these residues, Y197 is observed in KaDapE, PaDapE, and EcDapE but it is replaced by M and V in EfDapE and SaDapE, respectively (Fig. 8). These changes in residues apparently are not linked to differences in equilibrium binding experiments, since in these enzymes, the flavonoids do not enter the active site far enough to carry out additionally interactions or repulsions with the side chains of hydrophobic residues; N244 is found in ESKE-DapEs but is replaced by a T in PaDapE (Fig. 8A). In this enzyme the OH group of equivalent T, performs similar interactions as in the rest of model complexes; finally, N245 is missing in EfDapE and SaDapE and in all Gram-positive-DapE enzymes (Fig. 8A and C). (3) Relatively variable residues: S19 is replaced by N in most of the DapE of Gram-positive bacteria or in some cases to a D or L (Fig. 8C), the side chain of this N carries out polar interactions with the C ring O1 of rutin and hesperidin in SaDapE and with the OH 7 of rutin in HiDapE, KaDapE, EcDapE, while a replacement by a T in PaDapE allows similar interactions (Fig. 8A and B). N185 is replaced by a K in SaDapE and PaDapE, which in SaDapE it potentially makes important interactions only with the B ring and with the carbohydrate moiety of rutin, but it is not relevant for binding of other flavonoids. Y252 and Q254 are located in the oligomerization domain and are only observed stabilizing the carbohydrate moiety of rutin. Position 288 could be important to increase DapE interactions with flavonoids, since the presence of a W residue at this position seems to be related to a more favorable binding of these compounds (Fig. 8A and B). Finally, S290 that is changed to N in EfDapE and SaDapE (Fig. 8A), perform equivalent interactions in the respective enzyme-flavonoid complexes.

3.4. General discussion

DapE enzyme has been exhaustively investigated with the goal of finding potential inhibitory compounds, under the premise that they possess antibacterial properties. Such studies could provide insights of the molecular basis of the interactions, which are essential for the design and development of a new class of antibiotics [1,7,11,13]. The optimal type of inhibitors are those compounds that are harmless to humans and contain soft Lewis bases groups that are able to interact with the Zn^{2+} centers. In this regard, anti-DapE compounds previously described potentially re-purposed approved drugs that contain thiol groups, boronic acid derivatives, phenyl derivatives, phosphate derivatives [11,21]. Another promising inhibitors appear to be indoline sulfonamides [12,13], as shown by studies currently under patent application (PCT 62/036,346 nonprovisional filed August 12, 2015, and PCT 62/191,119, Nonprovisional PCT filed July 11, 2016). Previously, it was reported the high-resolution crystalline structure of a DapE in complex with L-captopril [7], a recognized inhibitor of this enzyme and that possesses a thiol group [7,11,21]. In the crystal, it was observed that the Zinc-Binding-Groups (ZBG) of L-captopril is linked between the two Zn^{2+}-centers of the *Neisseria meningitidis* DapE [7]. Subsequently, in another study of the *Salmonella enterica* DapE, replacement of Zn^{2+} ion by Mn^{2+} in the metallic center 2, resulted in the loss of inhibition by L-captopril [6], underlining the importance of metallic heterogeneity of an enzyme in the design and selection of relevant physiological inhibitors. This highlights that the metal center 2 of the DapE enzyme is important for the specificity of the ligand. Flavonoids are compounds of natural origin; mainly found in plants that are part of the human diet. Therefore, flavonoids are relatively harmless to human health and have been recognized as possessing an important role in formulating new strategies for the prevention and treatment of different diseases.

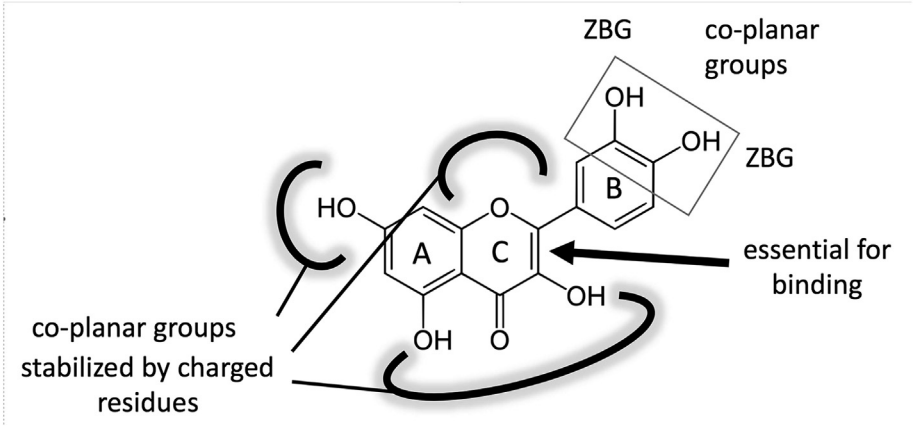

Fig. 9. General Structure of a Flavonoid. Important regions are marked. Structure was elaborated using ChemScketch®.

Flavonoids present numerous OH groups, which can chelate Zn^{2+}. These ZBGs are distributed in a characteristic pattern in a three-ring arrangement (Figs. 1 and 9), the ZBGs located in B ring are in the same plane due to its aromaticity. In the case of the flavonol and the flavones derivatives, the oxygen groups in A and C rings are also co-planar. Flavonoids are known protein ligands, as is the case of digestive enzymes [28–30], in urease [47,48], in human glyoxylase [49–51] and are now described as ligands of the DapE enzyme.

Experimental data and theoretical structural analyses of the binding of a selective group of flavonoids into the DapE enzymes of five biomedically relevant bacteria are presented. Among those, luteolin and rutin were identified in a virtual screening with the natural products database, which suggests a good correlation between inference by this virtual tool and experimental observations. Additionally, we selected quercetin, catechin, and hesperidin as model flavonoids, mainly due to their antimicrobial properties and our experience in previous studies with biomedically relevant digestive enzymes [28–30]. The structural details of these compounds are presented and in summary, the presence of MBG in a co-planar arrangement seems to be important for the recognition of these ligands by the active site of the DapE enzymes (Fig. 9). Concerning the DapE enzymes used in this study, were those that belong to four of the ESKAPE bacteria [26]. Two of these EfDapE and SaDapE are representative of Gram-positive organisms and three of Gram-negative bacteria, KaDapE, PaDapE, and EcDapE. Some differences were found at the biochemical level between these two groups of enzymes. Remarkably, there is a high agreement between the differences in binding equilibrium experiments and the structural aspects of enzyme-flavonoid complexes. In particular, these suggest modest contrasts between enzymes of Gram-positive and Gram-negative organisms (Figs. 4, 7, and 8). One significant difference is the presence of a substitution G324A in EfDapE that reduces the space for accommodation of flavonoid B ring in the active site cavity. This suggests that in some Gram-positive DapEs it is required relatively less bulky inhibitors to block the optimal function of the metal centers. The presence of aromatic residues, such as the case of a W at position 288 and F266, could account for an increased affinity for flavonoids, and probably for other potential inhibitors that present aryl groups. Although we found correlations between experimental and theoretical results, it is recommended that *in silico* predictions are further validated.

The HiDapE enzyme crystal in its closed form and in complex with the reaction products was recently resolved, showing the two stabilizing cationic groups of the oxyanion hole. One of these stabilizing groups is the Zn-2 center and the other is the imidazole of H195 side chain [23]. The substrate was also docked to identify relevant interacting amino acid residues required for the formation of the complex; and notably, substitution mutation of H195 showed its relevance for optimal catalytic activity [23]. This conformational transition of DapE enzymes and the interference with the oxyanion hole appear to be important architectural properties that could be exploited in the selection and development of anti-DapE agents [9,23]. In this sense, our observations from the docking studies suggest that flavonoids do not interfere with the closure of the enzyme (since their bindings are compatible in both the open and closed forms), but, through the interactions of the ligands with the metal center and with the H195, and consequently, we infer that flavonoid would block the correct functioning of the oxyanion hole (Fig. 5). We performed a NSDAP docking into the closed form to predict if the binding of the flavonoids is incompatible with the substrate binding and we found that they occupy exactly the same space (Fig. 6), thus, we infer a possible competitive mechanism of inhibition, however, more studies are required. Presumably, polyphenols could stimulate the conformational change in the enzyme from open to closed form, consistent with the large changes in fluorescence that we observed after binding of these ligands.

4. Conclusions

The anti-DapE compounds should possess: (1) One or more groups that participate in the binding with the metal centers in an arrangement similar to that of the NSDAP substrate, R1–C = O–NH–CH- (COOH) -R2, i.e. a ZBG attached to a trigonal carbon, followed by another adjacent ZBG and a third ZBG separated by a carbon and attached to another trigonal carbon. (2) Groups that can interact with the residues that are located in the cavity of the active site, both negatively (E134 and E163) and positively (R259, R329, H194, and H349) charged. (3) Relatively small main chains compatible with the enzyme conformational changes. In the flavonoids case, we found that the B ring is potentially the one that participates in the interaction with the metal centers, through the co-planar OH groups of the aromatic ring. The OH groups and the Oxo-4 group that are in the same plane in the flavonols and flavones are complementary to the residues at the active site. In the case of catechin, a flavan-3-ol that lacks double bond in C ring, its binding to DapE was not detected. Finally, flavonoid binding is compatible with both the open and closed forms of DapE.

The present study shows that flavonoids contain ZBG distributed in a pattern that allows their interaction with DapE enzymes. Derived from the observed data, it is inferred that ZBG attached to trigonal carbons are more suitable to interact with DapE.

Author contributions

Conception of the work: M.T-L., N.L-G., E.A-P., A.G.D-S.; collection of data: M.T-L., L.G.A-R., J.L.C-A., A.G.D-S.; analysis of data: M.T-L., N.L-G., E.A-P., L.dR., A.M-M., A.G.D-S. and writing of manuscript: M.T-L., N.L-G., E.A-P., A.G.D-S.

Declaration of competing interest

Regarding the following manuscript, we declare none conflict of interest.

Acknowledgements

Funding: This work was supported by the Nacional Council of Science and technology: "*Consejo Nacional de Ciencia y Tecnología*" (CONACYT) from the Government of Mexico, through the program "*Proyecto de Desarrollo Científico para Atender Problemas Nacionales*": [grant number CONACYT-PN-2015-587] and Ciencia Básica [grant number CONACYT-CB-2016-286449]; and by Universidad Autónoma de Ciudad Juárez. Manuel Terrazas-Lopez received a fellowship for a master's degree and another for a PhD degree by CONACYT-National Fellowship Program.

References

[1] D.M. Gillner, D.P. Becker, R.C. Holz, Lysine biosynthesis in bacteria: a metallodesuccinylase as a potential antimicrobial target, J. Biol. Inorg. Chem. 18 (2013) 155–163, https://doi.org/10.1007/s00775-012-0965-1.

[2] M. Karita, M.L. Etterbeek, M.H. Forsyth, M.K.R. Tummuru, M.J. Blaser, Characterization of *Helicobacter pylori* DapE and construction of a conditionally lethal DapE mutant, Infect. Immun. 65 (10) (1997) 4158–4164. https://iai.asm.org/content/65/10/4158.long.

[3] T.L. Born, R. Zheng, J.S. Blanchard, Hydrolysis of N -Succinyl-L, L -diaminopimelic acid by the *Haemophilus influenzae dapE* -encoded Desuccinylase : metal activation , solvent isotope effects , and kinetic mechanism, Biochemistry 2960 (1998) 10478–10487.

[4] N.R. Uda, M. Creus, Selectivity of inhibition of N-succinyl-L, L-diaminopimelic acid desuccinylase in Bacteria : the product of dapE-gene is not the target of L-captopril antimicrobial activity, Bioinorgan. Chem. Appl. 2011 (2011) 1–6, https://doi.org/10.1155/2011/306465.

[5] B. Nocek, A. Starus, M. Makowska-Grzyska, B. Gutierrez, S. Sanchez, R. Jedrzejczak, J.C. Mack, K.W. Olsen, A. Joachimiak, R.C. Holz, The dimerization domain in DapE enzymes is required for catalysis, PLoS One 9 (2014), https://doi.org/10.1371/journal.pone.0093593.

[6] N.R. Uda, G. Upert, G. Angelici, S. Nicolet, T. Schmidt, T. Schwede, M. Creus, Zinc-selective inhibition of the promiscuous bacterial amide-hydrolase DapE: implications of metal heterogeneity for evolution and antibioticdrug design, Metall 6 (2014) 88–95, https://doi.org/10.1039/C3MT00125C.

[7] A. Starus, B. Nocek, B. Bennett, J.A. Larrabee, D.L. Shaw, W. Sae-Lee, M.T. Russo, D.M. Gillner, M. Makowska-Grzyska, A. Joachimiak, R.C. Holz, Inhibition of the dapE-encoded N-Succinyl-L,L-diaminopimelic acid desuccinylase from *Neisseria meningitidis* by L-captopril, Biochemistry 54 (2015) 4834–4844, https://doi.org/10.1021/acs.biochem.5b00475.

[8] V. Usha, A.J. Lloyd, D.I. Roper, C.G. Dowson, G. Kozlov, K. Gehring, S. Chauhan, H.T. Imam, C.A. Blindauer, G.S. Besra, Reconstruction of diaminopimelic acid biosynthesis allows characterisation of *Mycobacterium tuberculosis* N-succinyl-L,L-diaminopimelic acid desuccinylase, Sci. Rep. 6 (2016) 23191, https://doi.org/10.1038/srep23191.

[9] D. Dutta, S. Mishra, Structural and mechanistic insight into substrate binding from the conformational dynamics in apo and substrate-bound DapE enzyme, Phys. Chem. Chem. Phys. 18 (2016) 1671–1680, https://doi.org/10.1039/C5CP06024A.

[10] D. Dutta, S. Mishra, Active site dynamics in substrate hydrolysis catalyzed by DapE enzyme and its mutants from hybrid QM/MM-Molecular dynamics simulation, J. Phys. Chem. B 121 (2017) 7075–7085, https://doi.org/10.1021/acs.jpcb.7b04431.

[11] D. Dutta, S. Mishra, L-Captopril and its derivatives as potential inhibitors of microbial enzyme DapE: a combined approach of drug repurposing and similarity screening, J. Mol. Graph. Model. 84 (2018) 82–89, https://doi.org/10.1016/j.jmgm.2018.06.004.

[12] T.K. Heath, The Enzymatic Activity and Inhibition of DapE Encoded N-Succinyl-L,l-Diaminopimelic Acid Dessucinylase, Loyola University Chicago, 2018. https://ecommons.luc.edu/luc_diss/2811/.

[13] T.K. Heath, M.R. Lutz, C.T. Reidl, E.R. Guzman, C.A. Herbert, B.P. Nocek, R.C. Holz, K.W. Olsen, M.A. Ballicora, D.P. Becker, Practical spectrophotometric assay for the *dapE*-encoded N-succinyl-L,L-diaminopimelic acid desuccinylase, a potential antibiotic target, PLoS One 13 (2018), e0196010, https://doi.org/10.1371/journal.pone.0196010.

[14] F. Javid-Majd, J.S. Blanchard, Mechanistic analysis of the *argE*-encoded N-acetylornithine deacetylase, Biochemistry 39 (2000) 1285–1293, https://doi.org/10.1021/bi992177f.

[15] N.J. Cosper, D.L. Bienvenue, J.E. Shokes, D.M. Gilner, T. Tsukamoto, R.A. Scott, R.C. Holz, The dapE-encoded N-Succinyl-L,L-Diaminopimelic acid desuccinylase from *Haemophilus influenzae* is a dinuclear metallohydrolase, J. Am. Chem. Soc. 125 (2003) 14654–14655, https://doi.org/10.1021/ja036650v.

[16] D.H. Broder, C.G. Miller, DapE can function as an aspartyl peptidase in the presence of Mn^{2+}, J. Bacteriol. 185 (2003) 4748–4754, https://doi.org/10.1128/JB.185.16.4748-4754.2003.

[17] R. Davis, D. Bienvenue, S.I. Swierczek, D.M. Gilner, L. Rajagopal, B. Bennett, R.C. Holz, Kinetic and spectroscopic characterization of the E134A- and E134D-altered *dapE*-encoded N-succinyl-l,l-diaminopimelic acid desuccinylase from *Haemophilus influenzae*, J. Biol. Inorg. Chem. 11 (2006) 206–216, https://doi.org/10.1007/s00775-005-0071-8.

[18] B.P. Nocek, D.M. Gillner, Y. Fan, R.C. Holz, A. Joachimiak, Structural basis for catalysis by the mono- and dimetalated forms of the *dapE*-encoded N-succinyl-l,l-Diaminopimelic acid desuccinylase, J. Mol. Biol. 397 (2010) 617–626, https://doi.org/10.1016/j.jmb.2010.01.062.

[19] Y. Tao, J.E. Shokes, W.C. McGregor, R.A. Scott, R.C. Holz, Structural characterization of Zn(II)-, Co(II)-, and Mn(II)-loaded forms of the *argE*-encoded N-acetyl-L-ornithine deacetylase from *Escherichia coli*, J. Inorg. Biochem. 111 (2012) 157–163, https://doi.org/10.1016/j.jinorgbio.2012.02.005.

[20] W.C. McGregor, D.M. Gillner, S.I. Swierczek, D. Liu, R.C. Holz, Identification of a histidine metal ligand in the *argE*-encoded N-Acetyl-L-Ornithine deacetylase from *Escherichia coli*, SpringerPlus 2 (2013) 482, https://doi.org/10.1186/2193-1801-2-482.

[21] D. Gillner, N. Armoush, R.C. Holz, D.P. Becker, Inhibitors of bacterial N-succinyl-l,l-diaminopimelic acid desuccinylase (DapE) and demonstration of in vitro antimicrobial activity, Bioorg. Med. Chem. Lett 19 (2009) 6350–6352, https://doi.org/10.1016/j.bmcl.2009.09.077.

[22] D.L. Bienvenue, D.M. Gilner, R.S. Davis, B. Bennett, R.C. Holz, Substrate specificity, metal binding properties, and spectroscopic characterization of the DapE-encoded N -succinyl-L, L-diaminopimelic acid desuccinylase from *Haemophilus influenzae*, Biochemistry 42 (2003) 10756–10763, https://doi.org/10.1021/bi034845+.

[23] B. Nocek, C. Reidl, A. Starus, T. Heath, D. Bienvenue, J. Osipiuk, R. Jedrzejczak, A. Joachimiak, D.P. Becker, R.C. Holz, Structural evidence of a major conformational change triggered by substrate binding in DapE enzymes: impact on the catalytic mechanism, Biochemistry 57 (2018) 574–584, https://doi.org/10.1021/acs.biochem.7b01151.

[24] A.T. Brunger, D. Das, A.M. Deacon, J. Grant, T.C. Terwilliger, R.J. Read, P.D. Adams, M. Levitt, G.F. Schröder, Application of DEN refinement and automated model building to a difficult case of molecular-replacement phasing: the structure of a putative succinyl-diaminopimelate desuccinylase from *Corynebacterium glutamicum*, Acta Crystallogr. Sect. D Biol. Crystallogr. 68 (2012) 391–403, https://doi.org/10.1107/S090744491104978X.

[25] J. Badger, J.M. Sauder, J.M. Adams, S. Antonysamy, K. Bain, M.G. Bergseid, S.G. Buchanan, M.D. Buchanan, Y. Batiyenko, J.A. Christopher, S. Emtage, A. Eroshkina, I. Feil, E.B. Furlong, K.S. Gajiwala, X. Gao, D. He, J. Hendle, A. Huber, K. Hoda, P. Kearins, C. Kissinger, B. Laubert, H.A. Lewis, J. Lin, K. Loomis, D. Lorimer, G. Louie, M. Maletic, C.D. Marsh, I. Miller, J. Molinari, H.J. Muller-Dieckmann, J.M. Newman, B.W. Noland, B. Pagarigan, F. Park, T.S. Peat, K.W. Post, S. Radojicic, A. Ramos, R. Romero, M.E. Rutter, W.E. Sanderson, K.D. Schwinn, J. Tresser, J. Winhoven, T.A. Wright, L. Wu, J. Xu, T.J.R. Harris, Structural analysis of a set of proteins resulting from a bacterial genomics project, Proteins Struct. Funct. Bioinforma. 60 (2005) 787–796, https://doi.org/10.1002/prot.20541.

[26] L.B. Rice, Federal funding for the study of antimicrobial resistance in nosocomial pathogens: No ESKAPE, J. Infect. Dis. 197 (2008) 1079–1081, https://doi.org/10.1086/533452.

[27] S.L. Percival, D.W. Williams, Escherichia coli, in: Microbiol. Waterborne Dis., Elsevier, 2014, pp. 89–117, https://doi.org/10.1016/B978-0-12-415846-7.00006-8.

[28] A.I. Martinez-Gonzalez, E. Alvarez-Parrilla, Á.G. Díaz-Sánchez, L.A. de la Rosa, J.A. Núñez-Gastélum, A.A. Vazquez-Flores, G.A. Gonzalez-Aguilar, *In vitro* inhibition of pancreatic lipase by polyphenols: a kinetic, Fluorescence spectroscopy and molecular docking study, Food Technol. Biotechnol. 55 (2017) 519–530, https://doi.org/10.17113/ftb.55.04.17.5138.

[29] A.I. Martinez-Gonzalez, Á.G. Díaz-Sánchez, L.A. De La Rosa, C.L. Vargas-Requena, I. Bustos-Jaimes, E. Alvarez-Parrilla, Polyphenolic compounds and digestive enzymes: *in vitro* non-covalent interactions, Molecules 22 (2017), https://doi.org/10.3390/molecules22040669.

[30] A.I. Martinez-Gonzalez, Á.G. Díaz-Sánchez, L.A. de la Rosa, I. Bustos-Jaimes, E. Alvarez-Parrilla, Inhibition of α-amylase by flavonoids: structure activity relationship (SAR), Spectrochim. Acta Part A Mol. Biomol. Spectrosc. 206 (2019) 437–447, https://doi.org/10.1016/j.saa.2018.08.057.

[31] M. De Carmen Pinto, A.L. Duque, P. Macías, Fluorescence quenching study on the interaction between quercetin and lipoxygenase, J. Fluoresc. (2011), https://doi.org/10.1007/s10895-010-0816-9.

[32] J. Huang, Z. Liu, Q. Ma, Z. He, Z. Niu, M. Zhang, L. Pan, X. Qu, J. Yu, B. Niu, Studies on the interaction between three small flavonoid molecules and bovine lactoferrin, BioMed Res. Int. (2018), https://doi.org/10.1155/2018/

7523165.
[33] V. Uivarosi, S.F. Barbuceanu, V. Aldea, C.C. Arama, M. Badea, R. Olar, D. Marinescu, Synthesis, spectral and thermal studies of new rutin vanadyl complexes, Molecules (2010), https://doi.org/10.3390/molecules15031578.
[34] L. Ni, F. Zhao, B. Li, T. Wei, H. Guan, S. Ren, Antioxidant and fluorescence properties of hydrogenolyzised polymeric proanthocyanidins prepared using SO_4^{2-}/ZrO_2 solid superacids catalyst, Molecules (2018), https://doi.org/10.3390/molecules23102445.
[35] J.J. Irwin, B.K. Shoichet, M.M. Mysinger, N. Huang, F. Colizzi, P. Wassam, Y. Cao, Automated docking screens: a feasibility study, J. Med. Chem. 52 (2009) 5712–5720, https://doi.org/10.1021/jm9006966.
[36] J.J. Irwin, T. Sterling, M.M. Mysinger, E.S. Bolstad, R.G. Coleman, ZINC: a free tool to discover chemistry for biology, J. Chem. Inf. Model. (2012), https://doi.org/10.1021/ci3001277.
[37] O. Trott, A.J. Olson, AutoDock Vina, Improving the speed and accuracy of docking with a new scoring function, efficient optimization, and multithreading, J. Comput. Chem. 31 (2010) 455–461, https://doi.org/10.1002/jcc.21334.
[38] E.F. Pettersen, T.D. Goddard, C.C. Huang, G.S. Couch, D.M. Greenblatt, E.C. Meng, T.E. Ferrin, UCSF Chimera? A visualization system for exploratory research and analysis, J. Comput. Chem. 25 (2004) 1605–1612, https://doi.org/10.1002/jcc.20084.
[39] A. Waterhouse, M. Bertoni, S. Bienert, G. Studer, G. Tauriello, R. Gumienny, F.T. Heer, T.A.P. De Beer, C. Rempfer, L. Bordoli, R. Lepore, T. Schwede, SWISS-MODEL: homology modelling of protein structures and complexes, Nucleic Acids Res. (2018), https://doi.org/10.1093/nar/gky427.
[40] C.B. Jalkute, S.H. Barage, M.J. Dhanavade, K.D. Sonawane, Identification of angiotensin converting enzyme inhibitor: an *in silico* perspective, Int. J. Pept. Res. Therapeut. 21 (2015) 107–115, https://doi.org/10.1007/s10989-014-9434-8.
[41] K. Anbarasu, S. Jayanthi, Designing and optimization of novel human LMTK3 inhibitors against breast cancer–a computational approach, J. Recept. Signal Transduct. Res. 37 (2017) 51–59, https://doi.org/10.3109/10799893.2016.1155069.
[42] S. Wang, J. Yao, B. Zhou, J. Yang, M.T. Chaudry, M. Wang, F. Xiao, Y. Li, W. Yin, Bacteriostatic effect of quercetin as an antibiotic alternative *in vivo* and its antibacterial mechanism in vitro, J. Food Protect. 81 (2018) 68–78, https://doi.org/10.4315/0362-028X.JFP-17-214.
[43] P.W. Taylor, J.M.T. Hamilton-Miller, P.D. Stapleton, Antimicrobial properties of green tea catechins, Food Sci. Technol. Bull. Funct. Foods 2 (2005) 71–81, https://doi.org/10.1616/1476-2137.14184.
[44] Y. Guo, Y. Liu, Z. Zhang, M. Chen, D. Zhang, C. Tian, M. Liu, G. Jiang, The antibacterial activity and mechanism of action of luteolin against *Trueperella pyogenes*, Infect. Drug Resist. 13 (2020) 1697–1711, https://doi.org/10.2147/IDR.S253363.
[45] N. Rani, C. Kumar, A. Arunachalam, L. PTV, Rutin as a potential inhibitor to target peptidoglycan pathway of *Staphylococcus aureus* cell wall synthesis, Clin. Microbiol. Infect. Dis. 3 (2018), https://doi.org/10.15761/cmid.1000142.
[46] A.S.A. Abuelsaad, I. Mohamed, G. Allam, A.A. Al-Solumani, Antimicrobial and immunomodulating activities of hesperidin and ellagic acid against diarrheic *Aeromonas hydrophila* in a murine model, Life Sci. 93 (2013) 714–722, https://doi.org/10.1016/j.lfs.2013.09.019.
[47] Á.G. Díaz-Sánchez, E. Alvarez-Parrilla, A. Martínez-Martínez, L. Aguirre-Reyes, J.A. Orozpe-Olvera, M.A. Ramos-Soto, A.J. Núñez-Gastélum, B. Alvarado-Tenorio, L.A. De La Rosa, Inhibition of urease by disulfiram, an FDA-approved thiol reagent used in humans, Molecules 21 (2016), https://doi.org/10.3390/molecules21121628.
[48] L.V. Modolo, A.X. de Souza, L.P. Horta, D.P. Araujo, Â. de Fátima, An overview on the potential of natural products as ureases inhibitors: a review, J. Adv. Res. 6 (2015) 35–44, https://doi.org/10.1016/j.jare.2014.09.001.
[49] R. Takasawa, K. Saeki, A. Tao, A. Yoshimori, H. Uchiro, M. Fujiwara, S.I. Tanuma, Delphinidin, a dietary anthocyanidin in berry fruits, inhibits human glyoxalase i, Bioorg. Med. Chem. 18 (2010) 7029–7033, https://doi.org/10.1016/j.bmc.2010.08.012.
[50] R. Takasawa, S. Takahashi, K. Saeki, S. Sunaga, A. Yoshimori, S. ichi Tanuma, Structure-activity relationship of human GLO I inhibitory natural flavonoids and their growth inhibitory effects, Bioorg. Med. Chem. 16 (2008) 3969–3975, https://doi.org/10.1016/j.bmc.2008.01.031.
[51] R. Takasawa, A. Tao, K. Saeki, N. Shionozaki, R. Tanaka, H. Uchiro, S. Takahashi, A. Yoshimori, S.I. Tanuma, Discovery of a new type inhibitor of human glyoxalase i by myricetin-based 4-point pharmacophore, Bioorg. Med. Chem. Lett 21 (2011) 4337–4342, https://doi.org/10.1016/j.bmcl.2011.05.046.